

Radiation Testing of GLAST LAT Tracker ASICs

R. Rando, A. Bangert, D. Bisello, A. Candelori, P. Giubilato, M. Hirayama, R. Johnson, H. F.-W. Sadrozinski, *Senior Member, IEEE*, M. Sugizaki, J. Wyss, and M. Ziegler

Abstract—Gamma-ray large area space telescope (GLAST) is a next generation high-energy gamma-ray space observatory designed for observations of celestial gamma-ray sources in the energy band extending from 10 MeV to more than 100 GeV. The main instrument, the large area telescope (LAT), consists of a microstrip silicon tracker, a calorimeter, an anticoincidence detector, and the data acquisition (DAQ) system. This paper summarizes the results obtained during the radiation testing of the ASIC chips used in the LAT tracker. Both single event effects (SEE) and total ionizing dose effect (TID) tests have been performed, as part of the radiation hardness assurance (RHA) for the planned 5-yr mission. Heavy-ion SEE tests have been performed at the SIRAD irradiation facility at the INFN National Laboratories of Legnaro, Italy (LNL) and at the Texas A&M University (TAMU) Cyclotron Institute, with LET values ranging up to $\sim 80 \text{ MeV} \times \text{cm}^2/\text{mg}$. The tolerance of the chips to ionizing radiation has been evaluated with heavy ions and by irradiating chips with the spherical ^{60}Co gamma source of the LNL CNR-ISOF laboratory.

Index Terms—Gamma-ray effects, ion radiation effects, radiation effects.

I. INTRODUCTION

GALACTIC and extragalactic gamma-ray sources are of great interest to both high-energy astrophysics and particle physics. Telescopes capable of studying the highest energy gamma-ray emissions play an important role thanks to their broad multiwavelength sky coverage capabilities. NASA's EGRET experiment on the Compton Gamma Ray Observatory [1] revolutionized the field of gamma-ray astronomy; its success and the new questions it posed demanded a follow-up mission with widely expanded capabilities. The large area telescope (LAT) [2], [3] on the gamma-ray large area space telescope (GLAST) is a next generation gamma-ray pair conversion telescope that makes use of silicon-strip detector technology [4]. It will observe celestial gamma-ray sources in the energy range from 20 MeV to 300 GeV with a field of view greater than 2 steradians. Compared to EGRET, the sensitivity of LAT will be improved by a factor of 50 or more: this is accomplished primarily by taking advantage of the silicon-strip

detectors which provide nearly 100% detection efficiency for charged particles, optimal angular resolution, small dead time, excellent multitrack separation, and self-triggering capability. Silicon-strip detector technology is known to be robust, requires no consumables, and operates at a relatively low voltage, all of which are ideal features for space applications.

The LAT is subdivided into four interdependent subsystems: tracker (TKR), calorimeter (CAL), anticoincidence detector (ACD), and data acquisition (DAQ) system. The TKR, composed of layers of silicon strip detectors, is placed on top of the CsI CAL; the whole TKR-CAL assembly is surrounded by a plastic segmented ACD. The tungsten foils preceding the detector planes in the TKR convert the incident gamma-ray photons into electron-positron pairs, which are then tracked by the silicon layers to determine the photon direction. Finally, the CAL absorbs the secondary particles and thereby measures the primary photon energy. Data collection and management is performed by the DAQ. A schematic representation of the LAT is shown in Fig. 1.

II. TKR ELECTRONICS

The GLAST LAT detector is highly modular: it consists of 16 tower modules, each of which has an 18-layer TKR, the CsI CAL, and the tower electronic module (TEM) readout electronics. In the TKR, each silicon layer is constituted by four single-sided ladders placed in parallel, each made up by four single-sided sensors; two such silicon layers, oriented at 90 degrees with respect to each other, are contained in each TKR tray (see Fig. 1). Each silicon detector has 384 strips and $8.95 \times 8.95 \text{ cm}^2$ active area; thus, the whole tracker has a total silicon surface of about 83 m^2 , segmented into almost 885 k channels.

Each silicon layer is connected through a pitch adapter to a hybrid multichip module (MCM), containing the layer readout ASICs plus some standard surface-mount electronic components to provide appropriate biasing and power. The readout is implemented using two ASICs, produced in Agilent $0.5\text{-}\mu\text{m}$ CMOS technology. The GLAST LAT front end (GTFE) ASICs are composed of an analog part (amplifier-shaper-threshold; 64 channels) plus the digital blocks for digitalization and communication [5], [6]. Satellite operations require low power consumption, due to the limited power provided by solar panels and to heat transfer requirements; such constraints dictate that the tracker readout electronics should not consume more than $\sim 240 \mu\text{W}$ per channel. Pulse-size analysis is not needed for GLAST, so power restrictions naturally lead to a binary readout with a simple single-threshold discriminator for each channel. A fast trigger is generated easily by calculating the logical OR of all GTFE channels in each layer.

Manuscript received November 14, 2003; revised February 12, 2004.

R. Rando, D. Bisello, A. Candelori, and P. Giubilato are with the Istituto Nazionale di Fisica Nucleare and the Dipartimento di Fisica, Università di Padova, I-35131 Padova, Italy (e-mail: rando@pd.infn.it; bisello@pd.infn.it; candelori@pd.infn.it; giubilato@pd.infn.it).

A. Bangert, M. Hirayama, R. Johnson, H. F.-W. Sadrozinski, M. Sugizaki, and M. Ziegler are with the Santa Cruz Institute for Particle Physics, University of California, Santa Cruz, CA 95064 USA (e-mail: myrtreia@yahoo.com; hirayama@scipp.ucsc.edu; johnson@scipp.ucsc.edu; hartmut@scipp.ucsc.edu; sugizaki@scipp.ucsc.edu; ziegler@scipp.ucsc.edu).

J. Wyss is with DIMSAT, Facoltà di Ingegneria, Università di Cassino, I-03043, Cassino (FR), Italy (e-mail: wyss@unicas.it) and also with the Istituto Nazionale di Fisica Nucleare, I-56100 Pisa, Italy.

Digital Object Identifier 10.1109/TNS.2004.829578

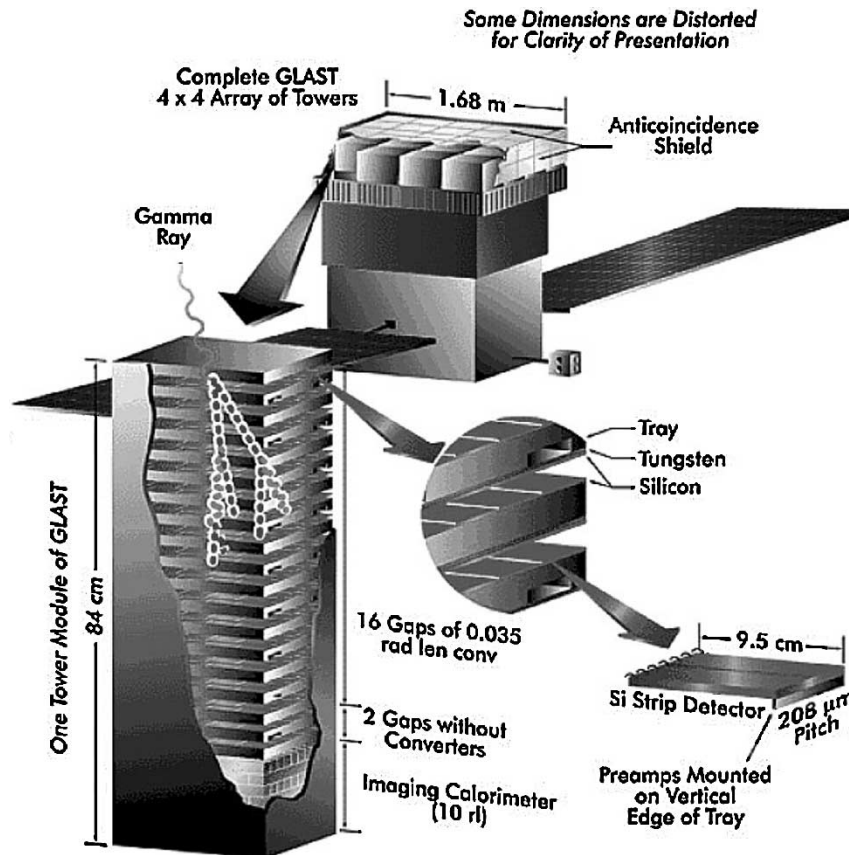


Fig. 1. Schematic representation of the GLAST LAT.

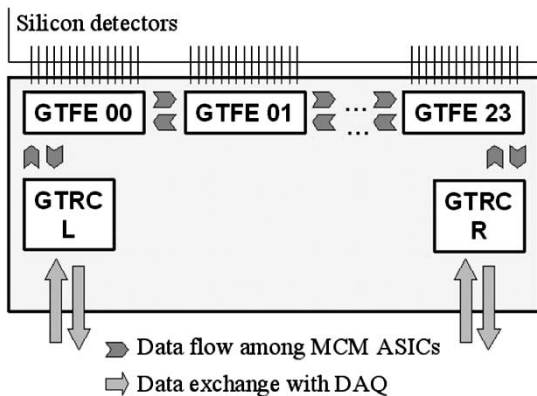


Fig. 2. Schematic representation of a TKR MCM.

Each MCM accommodates 24 GTFE ASICs, each connected to its neighbors to allow data transfer and trigger propagation. At both ends of this chain lies a GLAST LAT readout controller (GTRC) ASIC, a fully digital chip that interfaces the GTFEs with the DAQ electronics in the DAQ. A schematic representation of a TKR MCM is shown in Fig. 2. Taking into account the number of towers, layers, and channels in a layer, the authors obtain a total of 13 824 GTFEs and 1 152 GTRCs in the whole TKR.

Each GTFE ASIC contains three 64-bit registers that enable-disable calibration pulse, datataking, and trigger generation capabilities for each channel (henceforth labeled CAL, CHN, and TRG, respectively). Another 14-bit register (DAC) sets calibration pulse and cutoff threshold levels, while a small, two-bit reg-

ister (DEAF) permits the selection of leftward and rightward readout and the switching off of a malfunctioning chip.

Each GTRC ASIC has two registers: REG (34 bits) has 22 bits used to store configuration parameters, 7 bits used as error and status flags, and 5 bits that enable the modification of specific parts of the configuration, while SYNC (5 bits) controls synchronization with the GTFEs.

III. RADIATION DAMAGE

Deployment in space exposes TKR ASICs to ionizing radiation and, consequently, to radiation induced damage, which can be classified into two categories: SEE, where the passage of a single ionizing particle causes an undesired process to occur within an ASIC, and total ionizing dose effects (TID) due to the cumulative action of ionizing radiation during a prolonged exposure.

Among all SEEs, the most relevant for the LAT are single event upsets (SEU) and single event latchup (SEL). In a SEU, a single particle releases enough charge in the proximity of a memory cell to change its status ($1 \rightarrow 0$ or $0 \rightarrow 1$), thus corrupting data or modifying the ASIC configuration. To limit the impact of these phenomena all registers in both GTFE and GTRC ASICs are SEU-hardened [7]. In a SEL, the energy released by a single particle is injected into parasitic p-n-p-n structures inherent to CMOS technology, triggering a short-circuit that can lead to the destruction of the affected device.

The Agilent 0.5- μ m CMOS process is relatively radiation hard, being based on an epitaxial structure; the thickness of the

processed layer is about 13 μm including the epitaxial layer. This technology has already been shown to be SEU resistant to heavy ions [8]. The purpose of this paper is to demonstrate radiation hardness assurance (RHA) for the LAT TKR flight ASICs.

IV. TKR RADIATION ENVIRONMENT

GLAST will be in a low Earth orbit, at an altitude of 565 km and an inclination of 28.5 degrees [9]. The instrumentation will be consequently shielded from a large portion of the space radiation. The orbit will, however, intersect the South Atlantic Anomaly (SAA) which will give the most important contribution to total dose.

The radiation environment in which the telescope will operate is well understood [2], [9]. The spectra of galactic cosmic ray nuclei (GCR) are well represented by the CREME model; the solar particle (SPE) contribution is calculated, taking into account the modulation of solar activity and the corresponding atmospheric influence on the magnetic belts. Albedo from charged particles interacting with Earth's atmosphere is described by data collected during previous experiments.

The expected total ionizing dose is due to trapped protons in the SAA. The accumulated TID in a 5-yr mission is about 0.8 krd in the TKR outer layers. Allowing for a factor five engineering margin, we obtain about 4 krd; we required testing of all ASICs up to 10 krd to allow for an overall margin of 12.5 times the expected radiation levels. All dose values reported in this paper are referred to silicon.

For SEE issues we will consider GCR and SPE, taking into account the linear energy transfer (LET) at the surface of silicon. For GCR, we can estimate an upper energy cutoff at around $28 \text{ MeV} \times \text{cm}^2/\text{mg}$, while for SPE the limit is about $100 \text{ MeV} \times \text{cm}^2/\text{mg}$ [9].

Irradiation performed on analog-digital test structures containing four 32-bit registers indicates a SEE threshold of about $8 \text{ MeV} \times \text{cm}^2/\text{mg}$ [10]; since this threshold value is confirmed by the data presented in this report, the threshold will be held fixed to $8 \text{ MeV} \times \text{cm}^2/\text{mg}$ when fitting to simplify the convergence. Above this LET, we estimate a worst case scenario by multiplying the maximum possible particle flux in the planned 5 yr of operation by the total mission time, obtaining $\sim 0.2 \text{ ions}/\text{cm}^2$ due to GCR and $< 0.1 \text{ ions}/\text{cm}^2$ due to SPE in 5 yr. As a conservative upper limit, we will then assume a fluence of 1 ion/ cm^2 in 5 yr above the SEE LET threshold ($8 \text{ MeV} \times \text{cm}^2/\text{mg}$). For validation purposes, we require the expected number of upsets in the whole LAT in 5 yr to be smaller than about 700. As LAT configuration data will be reloaded periodically, this SEU rate is an acceptable safety factor to avoid an excessive data loss. Expected SELs, far more dangerous, must be less than 0.5 in 5 yr.

V. EXPERIMENTAL PROCEDURES

For the Radiation Hardness Assurance of TKR ASICs we first investigated several samples to understand their behavior after irradiation (SEE threshold, saturation, TID effects) [11]; the obtained results are reported in the following sections. The derived test plan is currently being applied in the screening phase (*validation*) for the ASIC flight lot, from which two GTFEs and two

TABLE I
ION SPECIES AT SIRAD

Ion Species	LET (MeV \times cm ² /mg)	Range in Si (μm)
²⁸ Si	8.5	62
⁵⁸ Ni	28.4	34
⁷⁹ Br	38.8	31
¹⁰⁷ Ag	54.7	28
¹⁹⁷ Au	81.7	23

TABLE II
ION SPECIES AT TAMU

Ion Species	LET (MeV \times cm ² /mg)	Range in Si (μm)
⁸⁴ Kr	27.8	134
¹²⁹ Xe	51.5	120

GTRCs were required to be tested for SEE effects and seven ASICs of each type for TID. All requirements are specified in [11], [12]; for all irradiations we used smaller area test-MCMs which can accommodate only seven GTFEs and two GTRCs.

Heavy ion irradiations were performed at the SIRAD beam line at the INFN National Laboratories of Legnaro (LNL), Italy [13]. A Tandem Van de Graaf 15-MV accelerator provides ion beams ranging from H to Au. A summary of the ion beams used for this study is reported in Table I. The surface LET values range from the aforementioned threshold ($8 \text{ MeV} \times \text{cm}^2/\text{mg}$) up to about $80 \text{ MeV} \times \text{cm}^2/\text{mg}$, well above the value when SEE saturation is expected from previous measurements on test structures [9] (around $35 \text{ MeV} \times \text{cm}^2/\text{mg}$).

To investigate a possible dependence of SEL cross sections on ion range, an additional SEE test was performed at the TAMU Cyclotron Institute [14]. The list of ions used is reported in Table II; in both cases the beam energy was set to 15 MeV/amu. For both Kr and Xe a first, low-flux [$10^4 \text{ ions}/(\text{cm}^2 \times \text{s})$] irradiation was carried out to obtain SEU cross sections to be compared with previous results from analog parts tested at SIRAD. Then a high-flux [$10^5 \text{ ions}/(\text{cm}^2 \times \text{s})$] irradiation was performed on four GTFE and four GTRC to calculate SEE cross sections. As can be seen in Tables I and II, the ranges of the ions we employed at TAMU are about four times greater than those used at SIRAD.

For TID, we used gamma rays from a 4π ⁶⁰Co source of the CNR-ISOF laboratory at LNL. Following standard ASTM and MIL procedures (see, for example, [15]) devices were placed within a Pb-Al box (wall thickness: 2.5 mm Al, 2 mm Pb) to eliminate low-energy photon and electron components that can lead to dose enhancement on the device under test (DUT) surface. Each DUT was powered and clocked during irradiation; uniformity and dose rate were experimentally verified before the validation phase started and were found to be as expected by geometrical considerations (dose rate 1 rd/s, uniformity better than 10% on a test-MCM).

Power during irradiation was provided by a custom-built power supply, designed to detect a SEL in less than 1 μs . A built-in serial interface allowed the user to monitor such events from a PC and log them together with other SEE/TID data.

TABLE III
ASIC FUNCTIONALITY TESTS

Test	Short Description
GTRC Register R/W	Load bit pattern in GTRC registers, read it back and check for errors.
GTFE Register R/W	Load bit pattern in GTFE registers, read it back and check for errors. Access GTFE individually.
GTFE Register Broadcast R/W	Load bit pattern in GTFE registers, read it back and check for errors. Broadcast commands.
GTRC Addressing	GTRC register R/W test, repeat for all possible GTRC layer IDs.
Hard and Soft Reset	Load non-default pattern in GTFE registers. Reset and read back pattern. Repeat for soft and hard reset.

TABLE IV
GTFE PERFORMANCE TESTS

Test	Short Description
Noise Rate	Measure noise rate on Layer-OR channel. No calibration strobe.
Readout with Charge Injection	Complete readout sequence, with calibration strobe. Repeat for all GTFE internal buffers. Check event buffer and Layer-OR.
Register Mask Tests	Disable all channels. Complete readout sequence, with calibration strobe. Check event buffer and Layer-OR to be empty.
Threshold Test with Charge Injection	Set threshold to Complete readout sequence, with calibration strobe. Check event buffer and Layer-OR.

Tests required for TID RHA are listed in Tables III–IV: functionality tests were selected to cover the basic digital capabilities of each ASIC, while performance tests focused on the GTFE analog front end. All tests were repeated before and after irradiation and results obtained were compared; it is assumed here that ASICs reaching the radiation validation phase operate properly (i.e., the relevant parameters are all within acceptable limits before irradiation).

In addition to the tests reported in Tables III and IV, power consumption was monitored to ensure that an eventual increase be smaller than 20%; no increase in power consumption due to radiation damage was observed.

Though not strictly required for RHA, a gain scan was always performed before and after irradiation for all tested GTFEs; this test was found to be useful in detecting radiation-induced changes in the GTFE behavior on a channel-by-channel basis. Gain in this context is defined as the threshold value for which a channel has 50% occupancy when calibration pulses and corresponding external triggers are issued. For each GTFE, CAL pulse heights were set, several calibration pulses were sent, and the corresponding occupancy was calculated.

More details, including ASIC configuration during tests and RHA requirements, can be found in [12].

VI. EXPERIMENTAL RESULTS: SEE

At SIRAD, for each ion beam the irradiation was divided into two parts: in the first we wrote in the registers a series of alternating 1s and 0s (“picket fence” pattern), waited for 10 s, read

TABLE V
SEU CROSS SECTIONS [$\text{cm}^2/(\text{ION} \times \text{BIT})$] AT SIRAD

LET [$\text{MeV} \times \text{cm}^2/\text{mg}$]	σ_{CAL} ($\times 10^{-8}$)	σ_{TRG} ($\times 10^{-8}$)	σ_{CHN} ($\times 10^{-8}$)	σ_{CONF} ($\times 10^{-8}$)
8.5	< 0.1	< 0.1	< 0.1	0.4±0.2
28.4	10.4±1.4	11.3±1.5	9.8±1.4	6.4±1.7
38.8	9.6±1.6	12.8±1.8	7.6±1.4	11.4±2.5
54.7	31.6±3.5	16.4±2.5	17.2±2.6	19.7±3.9
81.7	20.3±2.8	17.6±2.6	19.1±2.7	24.5±4.7

TABLE VI
SEU WEIBULL FIT PARAMETERS AT SIRAD

Register	S [$\times 10^{-7} \text{cm}^2/$ (bit ion)]	L_0 (fixed) [$\text{MeV} \times \text{cm}^2/\text{mg}$]	W [$\text{MeV} \times \text{cm}^2/\text{mg}$]
$\sigma_{\text{SEU-CAL}}$	3.1±1.1	8	57±30
$\sigma_{\text{SEU-TRG}}$	1.8±0.3	8	22±8
$\sigma_{\text{SEU-CHN}}$	2.9±1.4	8	68±46
$\sigma_{\text{SEU-CONF}}$	1.7±0.2	8	25 (fixed)

back the registers, and checked for errors. During the second part, the pattern was substituted with its complementary.

In addition to SEUs, communication errors (CME) and single event functionality interrupts (SEFI) were monitored. CME were defined as events where there was a clear transmission error in data coming from the DUT, the problem being temporary; in contrast, after a SEFI, the DUT did not answer user requests, requiring a reset to restart operation.

The resultant SEU cross sections per bit as obtained in these irradiations are reported in Table V. The errors in Table V are inferred from the number of observed events given Poisson statistics; the error on the delivered fluence is negligible in comparison. GTFE DEAF and GTRC SYNC are ignored in this analysis since they are statistically less significant due to the limited number of bits they contain, while SEU tests for GTRC REG are limited to the last 22 bits (labeled CONF bits) as other bits have special functions. In Table VI, we report the parameters obtained fitting the SEU cross sections per ASIC with the Weibull function [16]

$$\sigma_{\text{SEU}}(L) = S \cdot \left(1 - \exp\left(-\frac{L - L_0}{W}\right) \right) \quad (1)$$

where L_0 is the threshold LET, $L > L_0$ is the ion LET, S is the saturation limiting value, and W is the curve width. Fit curves and experimental data are shown in Fig. 3. For $\sigma_{\text{SEU-CONF}}$, we had to further constrain the fit to force convergence. As fit results had errors bigger than the corresponding parameter, we fixed the width W to the weighted average calculated for the GTFE registers; we thus have at least an estimate for the saturation limiting value of $\sigma_{\text{SEU-CONF}}$.

A saturation trend for SEU cross sections is observed in Fig. 3 after a LET of about $50 \text{ MeV} \times \text{cm}^2/\text{mg}$, corresponding to Ag. For this reason in the validation of flight parts, Au irradiations will not be performed.

CME and SEFI cross sections are given in Table VII. In Table VIII, we list the fit results: once again L_0 is fixed to $8 \text{ MeV} \times \text{cm}^2/\text{mg}$ to help the fit convergence. Results are not so good for GTRC CME: once again, errors were bigger than the parameters and the fit convergence was forced by

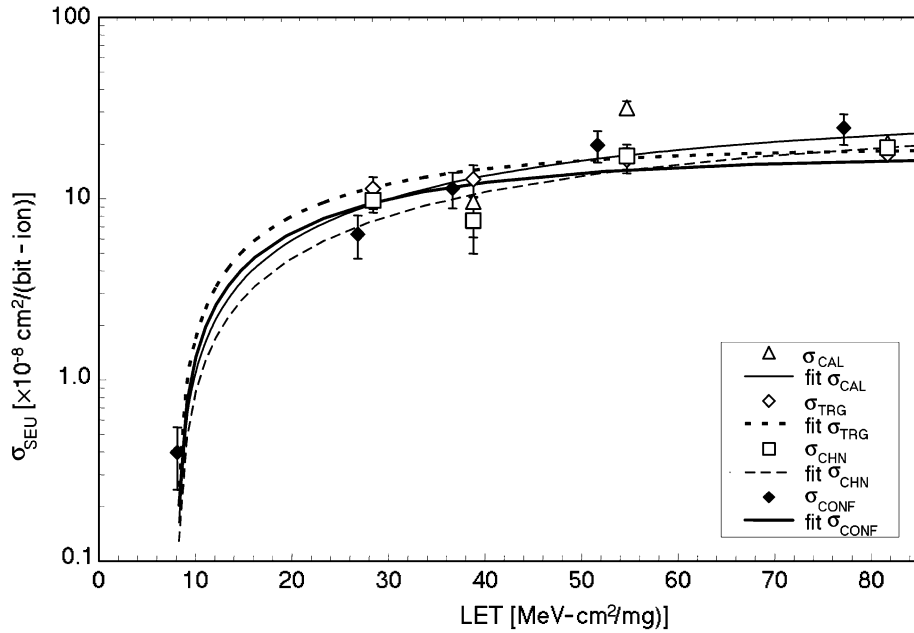


Fig. 3. Weibull fit of SEU cross sections. The plot data shown the three GTFE 64-bit registers, together with the CONF part of the GTRC REG register (i.e., the last 22 bits).

TABLE VII
CME-SEFI CROSS SECTIONS [$\text{cm}^2/(\text{ION} \times \text{ASIC})$] AT SIRAD

LET	$\sigma_{\text{CME-GTRC}}$ ($\times 10^{-7}$)	$\sigma_{\text{CME-GTFE}}$ ($\times 10^{-7}$)	$\sigma_{\text{SEFI-GTRC}}$ ($\times 10^{-7}$)	$\sigma_{\text{SEFI-GTFE}}$ at 95% C.L. ($\times 10^{-7}$)
8.5	2.9 ± 0.6	0.3 ± 0.2	4.6 ± 0.8	< 0.6
28.4	11.0 ± 3.3	29.0 ± 5.4	14.0 ± 3.7	< 3.8
38.8	18.8 ± 4.8	27.5 ± 5.9	26.3 ± 5.7	< 5.0
54.7	36.7 ± 7.8	30.0 ± 7.1	41.7 ± 8.3	< 7.5
81.7	40.0 ± 8.9	22.0 ± 6.6	22.0 ± 6.6	< 7.5

TABLE VIII
CME-SEFI WEIBULL FIT PARAMETERS AT SIRAD

Register	S [$\times 10^{-7} \text{ cm}^2/\text{ion}$]	L_0 (fixed) [$\text{MeV} \times \text{cm}^2/\text{mg}$]	W [$\text{MeV} \times \text{cm}^2/\text{mg}$]
$\sigma_{\text{CME-GTFE}}$	32.0 ± 7.3	8	25 ± 11
$\sigma_{\text{CME-GTRC}}$	30.7 ± 3.7	8	25 (fixed)
$\sigma_{\text{SEFI-GTFE}}$	n.a.	n.a.	n.a.
$\sigma_{\text{SEFI-GTRC}}$	31 ± 10	8	28 ± 22

fixing the width to the value found for the GTFE CME cross section. SEFIs were not observed in GTFE chips: cross sections were calculated assuming an upper limit of three events (corresponding to 95% confidence level) for the considered ion fluence.

SEL upper limits are reported in Table IX. Notably no latches were observed even after 5×10^6 Au ions/ cm^2 on GTRC DUTs and 4×10^6 Au ions/ cm^2 on GTFEs.

Expected number and upper limits (where appropriate) of SEU, CME, SEFI, and SEL for the whole tracker for a mission lasting 5 yr are shown in Table X. Figures presented for CME and SEFI were overestimated by multiplying the saturation value in Table VIII from the cross section by the number of ions hitting the TKR electronics in 5 yr (1 ion/ cm^2). In the case of SEU, we have calculated the weighted average of all the

TABLE IX
SEL CROSS SECTIONS UPPER LIMITS [$\text{cm}^2/(\text{ION} \times \text{ASIC})$] AT SIRAD

ASIC	Delivered Au fluence (ions/ cm^2)	σ_{SEL} at 95% C.L. ($\times 10^{-7}$)
GTRC	5×10^6	< 6.0
GTFE	4×10^6	< 7.5

TABLE X
SEE IN A 5-YR MISSION, WHOLE TKR (SIRAD)

SEE	Expected in GTFE (U.L. where $<$)	Expected in GTRC (U.L. where $<$)
SEU	0.7	0.005
CME	0.04	0.004
SEFI	< 0.01	0.004
SEL	< 0.01	< 0.0007

S values in Table VI, including the one for $\sigma_{\text{SEU-CONF}}$, obtaining $\langle S \rangle = (1.77 \pm 0.16) \times 10^{-7} \text{ cm}^2/(\text{ion} \times \text{bit})$; even if $\sigma_{\text{SEU-CONF}}$ were excluded from the average we would obtain $\langle S' \rangle = (1.93 \pm 0.28) \times 10^{-7} \text{ cm}^2/(\text{ion} \times \text{bit})$, compatible with the former estimate within 1σ . To obtain the SEU estimates we multiplied this average saturation limit by the number of ions hitting the TKR in 5 yr and by the total number of bits in the considered ASIC; for GTRC we have ignored “special” bits in REG as a SEU occurring there will not change the behavior of the electronics.

The authors would like to remark that the figures referring to SEL are only upper limits, rather than the expected number of latches. In all calculations, we considered a TKR composed of 13 824 GTFEs and 1 152 GTRCs.

TABLE XI
SEU CROSS SECTIONS [$\text{cm}^2/(\text{ION} \times \text{BIT})$] AT TAMU

LET	σ_{CAL} ($\times 10^{-8}$)	σ_{TRG} ($\times 10^{-8}$)	σ_{CHN} ($\times 10^{-8}$)	σ_{CONF} ($\times 10^{-8}$)
27.8	5.6 ± 0.9	5.2 ± 0.9	5.9 ± 1.0	7.7 ± 1.9
51.5	31.7 ± 2.2	10.5 ± 1.3	8.9 ± 1.2	22.7 ± 3.2

TABLE XII
SEE IN A 5-YR MISSION, WHOLE TKR AT TAMU

SEE	U.L for SEL in GTFE	U.L for SEL in GTRC
SEL	$< 4.4 \times 10^{-4}$	$< 3.8 \times 10^{-5}$

VII. EXPERIMENTAL RESULTS: RANGE DEPENDENCE OF SEE EFFECTS

At TAMU we investigated a possible dependence of SEL cross sections on the ion range. With respect to previous measurements at SIRAD, ion ranges were increased by a factor of 4 while surface LET was kept the same.

First, we performed two low flux runs with Kr and Xe to find SEU cross sections and compare results with measurements taken at SIRAD. In Table XI, we report the result for the low-flux irradiations; the SEU cross sections therein demonstrate a good agreement with the corresponding data in Table V obtained for Ni and Ag. No influence of range on SEU cross section appear evident from these data.

Subsequently, we performed several high flux irradiations with Xe, up to a total delivered fluence of 9×10^7 ions/ cm^2 for each ASIC type; no latchup was observed. In Table XII, we calculated the corresponding upper limit (at 95% C.L.) on the expected SEL number for the whole TKR in a 5-yr mission; we employed the same procedure we discussed for SIRAD data.

Our results indicate no need to extend the range of ions beyond that available at SIRAD for the epitaxial Agilent $0.5 \mu\text{m}$ CMOS process. Thus, we confirm the correctness of the standard procedure that considers an ion range of approximately twice the epitaxial layer thickness to be adequate for SEL testing [17].

In conclusion, we have successfully demonstrated that, during the 5-yr mission planned for the GLAST experiment, the probability of suffering a SEL is less than 1 over 2000 at 95% confidence level. The probability of suffering a SEU, a CME or a SEFI is also reassuringly low.

VIII. EXPERIMENTAL RESULTS: TID

A subset of the test procedures used for ASIC screening on the wafers was selected to be employed for TID validation with ^{60}Co gamma rays. In [12], a detailed description of the performed tests is given.

Power consumption was monitored to look for an increase due to ionizing radiation; no significant increase after irradiation was observed, while fluctuations remained within 5%.

A series of functionality tests was performed on both GTRC and GTFE ASICs. Monitored functionalities include register access and modification and, for GTFE only, analog performances: noise, gain, threshold, and calibration pulse were thoroughly examined (see Tables III, IV). The entire test set was

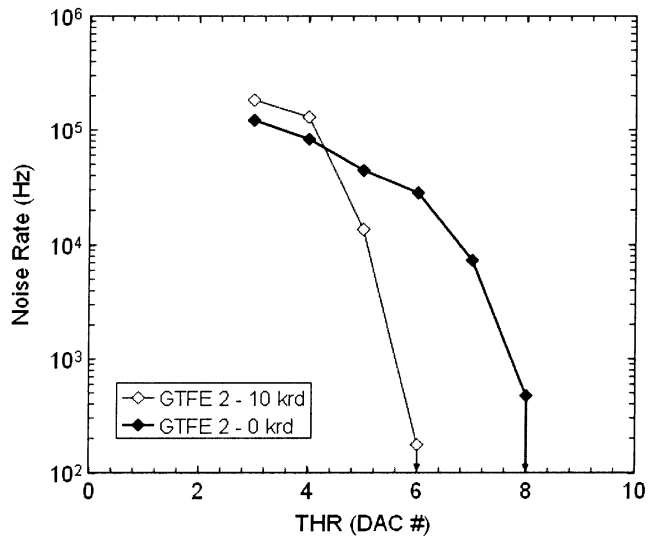


Fig. 4. Typical noise versus threshold curves for a GTFE, measured before and after ^{60}Co irradiation (delivered dose: 10 krd) on the OR channel. Arrows indicate the following point is equal to zero.

repeated before irradiation and after each 2.5 krd step up to a total of 10 krd. No significant change in DUT behavior was observed. As an example of TID tests, we will present some data about GTFE noise and gain: these are among the most interesting parameters, and those demonstrating the most evident changes after radiation, though remaining well within set limits.

In Fig. 4, a measurement of noise rate as a function of threshold level before and after irradiation is shown for a sample GTFE. The noise rate measurement is performed on the OR channel and the chip was not triggered, as the OR operation does not require it. Charge injection (calibration pulse) was not used: the measured noise is intrinsic to the front end. Validation requires the noise rate to be below 100 Hz per chip if the threshold is set to 10 (corresponding to 0.5 fC); this constraint was easily met by all GTFEs tested. Although it appears that noise rate increases at the lowest threshold values (below 5 DAC) due to ionizing radiation, at higher threshold values it actually decreases; this means that the equivalent noise charge (ENC) actually decreases with radiation. There are a few caveats in this analysis: the noise rate at very low thresholds is ill defined, and so high that saturation may occur; in addition, the threshold offsets or the shaping time might change slightly due to irradiation. A further, dedicated analysis of this behavior is required in order to understand it.

Noise tests performed on test prototype chips have shown that for the GTFE design the ENC can be parameterized in the usual way as

$$\text{ENC} = a + b \cdot C_{\text{IN}} \quad (2)$$

where a is about 150 electrons and b is about 22 electrons/pF. The input capacitance C_{IN} (i.e., the detector capacitance) is typically equal to 47 pF, so the amount of noise induced by the detector is at least 10 times greater than the ASIC intrinsic contribution. As can be seen in Fig. 4, the intrinsic chip noise a decreases after 10 krd. A measurement of the slope b for a GTFE, obtainable by connecting some capacitors (e.g., 24 and 48 pF)

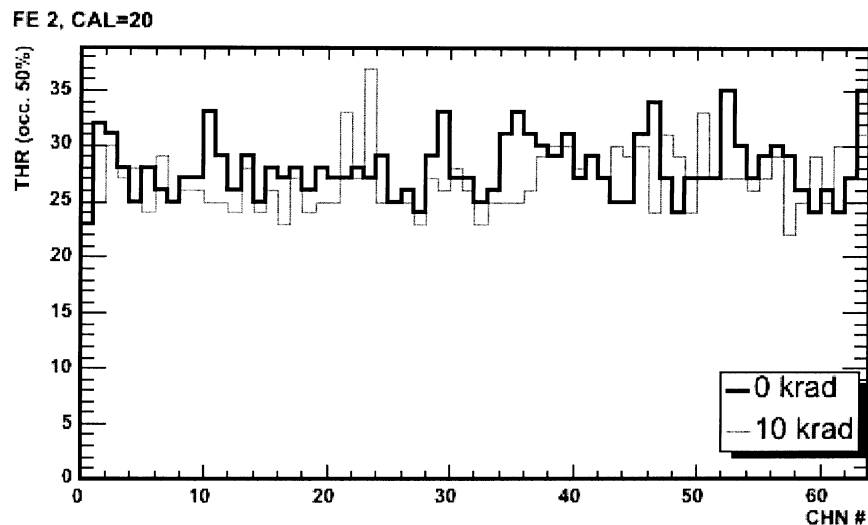


Fig. 5. Typical gain scan for a GTFE, measured before and after ^{60}Co irradiation (delivered dose: 10 krd).

to several input channels is being considered to understand the impact on the LAT on-orbit performance. In contrast, the tests presented here were performed to uncover gross effects in ASIC operation under vastly increased radiation levels.

Fig. 5 shows the typical result of a gain measurement performed on a GTFE, before and after ^{60}Co gamma irradiation. Data reported in Fig. 5 were obtained with a calibration pulse of 20 DACs, 100 pulses and corresponding external triggers were delivered for each threshold value and data acquired, starting from a threshold value low enough that all channels showed 100% occupancy, moving to higher threshold values and stopping when all channels were silent; the threshold value corresponding to 50% occupancy for each channel is plotted. Though a small change in the gain distribution is observed after irradiation, no systematic effect is evident.

All other functionality tests gave good results: we did not observe any problem due to radiation damage in all tested devices.

IX. CONCLUSION

We tested LAT TKR ASICs both for SEE and for TID effects. No catastrophic damage was observed in any tested device. The number of expected SEE events in the LAT TKR is negligible for the planned 5-yr mission, even considering that over 13 000 ASICs will be employed.

SEU and SEL results from SIRAD and TAMU irradiations, where the ion ranges differ by a factor of 4, are consistent with one another, indicating that an ion range much greater than three times the epitaxial layer thickness is not required.

In addition to the two types of LAT TKR ASICs described here, three LAT DAQ ASICs were tested at SIRAD with similar results, indicating very satisfactory radiation hardness for SEE and TID.

GLAST internal documents and technical reports can be accessed through the SLAC GLAST-LAT Document System [18].

REFERENCES

- [1] P. L. Nolan *et al.*, "Performance of the EGRET astronomical gamma ray telescope," *IEEE Trans. Nucl. Sci.*, vol. 39, pp. 993–996, Aug. 1992.
- [2] P. F. Michelson, "GLAST LAT," Stanford Univ., CA, Response to AO 99-OSS-03, 2002. E.
- [3] —, "GLAST: A detector for high-energy gamma rays," in *Proc. SPIE*, vol. 2806, Oct. 1996, pp. 31–40.
- [4] W. B. Atwood, J. A. Hernando, M. Hirayama, R. P. Johnson, W. Kröger, and H. F.-W. Sadrozinski, "The silicon tracker/convertor for the gamma-ray large-area space telescope," *Nucl. Instrum. Methods*, vol. A 435, no. 1–2, pp. 224–232, Oct. 1999.
- [5] R. P. Johnson, P. Poplevin, H. F.-W. Sadrozinski, and E. N. Spencer, "An amplifier-discriminator chip for the GLAST silicon-strip tracker," *IEEE Trans. Nucl. Sci.*, vol. 45, pp. 927–930, June 1998.
- [6] R. P. Johnson *et al.*, "The readout electronics for silicon tracker of the GLAST beam test engineering model," in *4th Int. Symp. Development and Application of Semiconductor Tracking Detectors*, Hiroshima, Japan, Mar. 2000. Presented.
- [7] L. R. Rockett, "An SEU-hardened CMOS data latch design," *IEEE Trans. Nucl. Sci.*, vol. 35, pp. 1682–1687, Dec. 1998.
- [8] J. V. Osborn, D. C. Mayer, R. C. Laco, S. C. Moss, and S. D. La Lumondiere, "Single event latchup characteristics of three commercial CMOS processes," in *Conf. Proc. 7th NASA Symp. VLSI Design*, 1998.
- [9] *GLAST Mission System Specification*, Oct. 2002. GSFC.
- [10] M. Sugizaki *et al.*, "SEE Test of the LAT Tracker Front End ASIC," SLAC, Menlo Park, CA, Tech. Rep. LAT-TD-00 333, 2001.
- [11] R. Rando and H. Sadrozinski, "Radiation Tests of GLAST LAT Electronic Components at LNL," SLAC, Menlo Park, CA, Tech. Rep. LAT-PS-01 059, 2002.
- [12] —, "Radiation Test Plan for the GLAST LAT TKR ASICs," SLAC, Menlo Park, CA, Tech. Rep. LAT-PS-01 325, 2003.
- [13] J. Wyss, D. Bisello, and D. Pantano, "SIRAD: An irradiation facility at the LNL tandem accelerator for radiation damage studies on semiconductor detectors and electronic devices and systems," *Nucl. Instrum. Methods*, vol. A 462, no. 3, pp. 426–434, Aug. 2001.
- [14] Texas A&M Univ. Cyclotron Institute, MS 3366, 77 843–3366, College Station, TX, USA.
- [15] *Standard Guide for Ionizing Radiation (Total Dose) Effects Testing of Semiconductor Devices*. ASTM guide, F 1892–98.
- [16] E. L. Petersen, J. C. Pickel, J. H. Adams, Jr., and E. C. Smith, "Rate prediction for single event effects—A critique," *IEEE Trans. Nucl. Sci.*, vol. 39, pp. 1577–1599, Dec. 1992.
- [17] A. H. Johnston, "The influence of VLSI technology evolution on radiation-induced latchup in space systems," *IEEE Trans. Nucl. Sci.*, vol. 43, pp. 505–521, Apr. 1996.
- [18] LATDocs: The SLAC GLAST-LAT Document System [Online]. Available: <http://www-glast.slac.stanford.edu/documents/LATDOCS.htm>